



Loss of HMBOX1 promotes LPS-induced apoptosis and inhibits LPS-induced autophagy of vascular endothelial cells in mouse

HanLin Ma^{1,2} · Le Su¹ · XiaoYing He¹ · JunYing Miao^{1,3}

Published online: 3 October 2019
© Springer Science+Business Media, LLC, part of Springer Nature 2019

Abstract

Our previous study revealed that Homeobox containing 1 (HMBOX1), essential for the survival of vascular endothelial cells (VECs), was involved in the progression of atherosclerosis. Knockdown of HMBOX1 promoted apoptosis and inhibited autophagy through regulating intracellular free zinc level in cultured VECs. In current study, in order to investigate the roles of HMBOX1 in vivo and in endothelium, we generated a knockout (KO) mouse for HMBOX1 by using transcription activator-like effector nucleases (TALENs) technology. Herein, we reported that the protein level of HMBOX1 was gradually increased during mouse development. The HMBOX1 KO mouse was viable and fertile. There existed no differences in apoptosis and autophagy of aortic endothelial cells between wild type and KO mouse. Whereas, loss of HMBOX1 promoted apoptosis and inhibited autophagy of aortic endothelial cells under lipopolysaccharide (LPS) stimulation in mouse. We also demonstrated that HMBOX1 deletion had no influence on the secretion of inflammatory cytokines TNF- α and IL-6. Moreover, overexpression or knockdown of HMBOX1 failed to regulate multiple pro-apoptotic genes expression in vitro. In conclusion, HMBOX1 participated in the functional maintenance of mouse aortic endothelial cells, the aortic endothelial cells of HMBOX1 KO mouse showed increased apoptosis and decreased autophagy with LPS treatment.

Keywords HMBOX1 · Knockout mouse · Endothelial cells · Lipopolysaccharide · Apoptosis · Autophagy

Abbreviations

ALT Alternative lengthening of telomeres
BMSC Bone marrow mesenchymal stem cell
ESC Embryonic stem cells
HMBOX1 Homeobox containing 1
HNF Hepatocyte nuclear factor

HUVEC Human umbilical vascular endothelial cell
LPS Lipopolysaccharide
MT2A Metallothionein 2A
TALEN Transcription activator-like effector nuclease
VEC Vascular endothelial cell
WT Wild type
KO Knockout

Electronic supplementary material The online version of this article (<https://doi.org/10.1007/s10495-019-01572-6>) contains supplementary material, which is available to authorized users.

✉ JunYing Miao
miaojy@sdu.edu.cn

- ¹ Shandong Provincial Key Laboratory of Animal Cells and Developmental Biology, School of Life Science, Shandong University, Qingdao 266237, People's Republic of China
- ² Department of Obstetrics and Gynecology, Qilu Hospital, Shandong University, Jinan 250012, People's Republic of China
- ³ The Key Laboratory of Cardiovascular Remodeling and Function Research, Chinese Ministry of Education and Chinese Ministry of Health, Shandong University Qilu Hospital, Jinan 250012, People's Republic of China

Introduction

Homeobox containing 1 (HMBOX1), a member of the homeobox transcription factor family, was first cloned from human pancreatic cDNA library in 2006 [1]. Studies had shown that HMBOX1 was involved in a variety of biological processes. In the beginning, HMBOX1 was demonstrated to participate in the immune and inflammation responses. HMBOX1 could negatively regulate natural killer (NK) cell function through inhibiting interferon- γ production and suppressing the NKG2D/DAP10 signaling pathway [2, 3]. Besides, miR-30c-1* enhanced NK cell cytotoxicity against hepatoma cells through targeting HMBOX1 [4]. Recent research showed that HMBOX1 activation inhibited

LPS-induced inflammation and ROS production by inhibition of NF- κ B and MAPK signal pathway [5]. A study in hepatocyte-specific HMBOX1 knockout mouse suggested that HMBOX1 could also rescue LPS/D-GalN-induced liver injury through inhibiting macrophage infiltration and activation [6].

HMBOX1 was also reported to support telomere elongation in telomerase-dependent and alternative lengthening of telomeres (ALT) cells by directly binding to double-stranded telomere repeats [7–9]. In addition, HMBOX1 performed diverse biological functions in different types of cancer, which was low-expression and inhibited malignant progression of glioma [10, 11], ovarian cancer [12] and liver cancer [13], but contributing to the poor prognosis of gastric cancer and radio-resistance of cervical cancer [14, 15]. We have been engaged in studying the functions of HMBOX1 in the differentiation and survival of vascular endothelial cells (ECs). Previously, we found that a small molecule 6-amino-2,3-dihydro-3-hydroxymethyl-1,4-benzoxazine (ABO) failed to induce rat bone marrow mesenchymal stem cells (BMSCs) and mouse embryonic stem cells (ESCs) differentiating into ECs without HMBOX1 [16, 17]. In addition, ABO elevated HMBOX1 expression by inhibiting the ANXA7 GTPase activity in vitro and in vivo [18]. More importantly, HMBOX1 could maintain the survival of human umbilical vascular endothelial cells (HUVECs) through promoting autophagy and inhibiting apoptosis [19]. Considering that HMBOX1 played such an important role in the formation and survival of HUVECs in vitro, we speculated that HMBOX1 might participate in the formation of ECs and the maintenance of EC functions in vivo.

Homeobox transcription factors played key roles in a vast range of biological processes including embryogenesis, organogenesis and angiogenesis [20, 21]. As one of the members, HMBOX1 was widely expressed in 18 human tissues, and highly conserved in human, mouse, rat, chicken and *Xenopus laevis*, indicating that HMBOX1 might participate in the development of mouse [1]. However, there are no appropriate mouse models to illustrate the roles of HMBOX1 in mouse development and EC functions in vivo.

In this study, to address these questions, we generated a knockout (KO) mouse for HMBOX1 using transcription activator-like effector nucleases (TALENs) technology and aimed to illuminate the functions of HMBOX1 in the formation and maintenance of EC functions in vivo.

Materials and methods

HMBOX1 knockout mouse construction

HMBOX1 knockout mouse (FVB/NJ background) was designed and constructed by View Solid Biotechnology

(Beijing, China). A targeted sequence near the ‘ATG’ code within the third exon of HMBOX1 gene (accession number: NM_177338.5) was chosen. TALEN-Left was designed against the sequence (5'-TTT CCC TCC AGT TTG CT-3') for the sense strand, and TALEN-right was designed against the sequence (5'-CTG GGT TCA TCT GTG T-3') for the anti-sense strand. The pair included bipartite 17 bp and 16 bp targeted sequences separated by a spacer region of 17 bp (5'-GGA AAC CAT GTC TCA CT-3').

Animals

All mice were housed under a 12 h light/dark cycle and pathogen-free conditions. Male mice between 2 and 3 months of age were used unless otherwise noted. Experiments were performed using groups of at least six animals. All efforts were made to minimize the suffering of animals.

Reagents and antibodies

Antibodies for HMBOX1 (sc-87768), GFP (sc-9996), CD31/PECAM-1 (sc-18916) and horseradish peroxidase-conjugated secondary antibodies were all from Santa Cruz Biotechnology (Dallas, TX, USA), β -actin (A5441) antibody was gained from Sigma-Aldrich (St. Louis, MO, USA), antibodies for LC3B (2775S), cleaved caspase-3 (9661S) and BIRC2 (baculoviral IAP repeat containing, 27065S) were from Cell Signaling Technology (Danvers, MA, USA), p62 (18420-1-AP) antibody was purchased from Proteintech Group (Wuhan, China). Secondary antibodies for immunofluorescence were Goat anti-Rabbit IgG Alexa Fluor-488 (A-11008) and Goat anti-Rat IgG Alexa Fluor-633 (A-21094, all Invitrogen, Waltham, MA, USA). The pCMV6-HMBOX1 plasmid was purchased from OriGene (SC319800, Rockville, MD, USA).

PCR-based genotyping

Genomic DNA was extracted from tail tips by proteinase K digestion. A portion of the HMBOX1 locus that overlaps the TALEN spacer region was amplified by RT-PCR. PCR reactions were performed using 2 \times EasyTaq PCR SuperMix (+ dye) (AS111, TransGen, Beijing, China) following the manufacturer's instructions. PCR products were analyzed by DNA sequence analysis using an anti-sense primer. Total RNA was isolated from fresh liver samples using TRIzol reagent (15596018, Invitrogen). An amount of 1 μ g RNA was reverse-transcribed into cDNA using a PrimeScript RT reagent Kit (RR037A, Takara, Kyoto, Japan). HMBOX1 cDNA was amplified as described above, followed by DNA sequence analysis. The primers used are shown in the supplementary information.

Quantitative real-time PCR (qRT-PCR)

qPCR was performed using the 7900HT Fast Real Time PCR System (Applied Biosystems, Waltham, MA, USA) with SYBR Premix Ex Taq (RR420A, Takara). The mRNA level of specific genes was normalized against β -actin using the comparative Ct method ($2^{-\Delta\Delta C_t}$). The primers used are shown in the supplementary information.

Cell lines and cell culture

Human aortic endothelial cells (HAECs) were obtained from the American Type Culture Collection (ATCC) and were grown in endothelial cell medium (ECM, 1001, ScienCell, Carlsbad, CA, USA) containing 5% fetal bovine serum (FBS) (16000-044, Gibco) and 1% endothelial cell growth supplement (1062, ScienCell). HAECs in passage of 3–8 were chosen for the experiments. HEK293T cells were obtained from the Cell Bank of the Chinese Academy of Sciences (Shanghai, China) and were grown in DMEM (Gibco, Grand Island, NY, USA) with 10% FBS.

RNA interference (RNAi)

Specific siRNA against BIRC2 (5'-AGG GAT ATA GTT TGA ATT CTA-3'), HMBOX1 (5'-AUU GAA GUA ACU UUC CAU AAC AGC C-3') and negative control siRNA were designed and synthesized by GenePharma (Shanghai, China). HAECs at 50% confluence were transfected with specific siRNA for 6 h using Lipofectamine 2000 reagent (11668-019, Invitrogen) according to the manufacturer's protocol, and then the transfection medium was replaced with culture medium. Gene silencing efficiency was detected by qRT-PCR or western blot.

Plasmid constructs

The coding region of HMBOX1 from WT or KO mouse was cloned into pEGFP-C2 expression vector to produce pEGFP-C2-WT and pEGFP-C2-KO plasmid, respectively. HEK293T cells were transfected with pEGFP-C2-WT and pEGFP-C2-KO using Lipofectamine 2000 reagent according to the manufacturer's protocol. 48 h after transfection, cells were harvested and subjected to western blot.

Western blot

In brief, as described previously [22], following separated by SDS-PAGE and transferred to PVDF membrane (IPVH00010, Merck Millipore, Burlington, MA, USA), proteins were probed with primary antibodies, then horseradish

peroxidase-linked secondary antibodies, and detected with the use of an enhanced chemiluminescence detection kit (ORT2655, PerkinElmer, Waltham, MA, USA).

En face staining

After fixed with 4% paraformaldehyde for 20 min and permeabilization with 0.2% Triton X-100 for 10 min, the ascending aorta and proximal arch segment were incubated with 10% donkey serum for 30 min at room temperature. Each aortic arch was then incubated simultaneously with primary antibodies, followed by the appropriate combination of secondary antibodies. The nuclei were stained with DAPI. For negative controls, segments were incubated with normal IgG. TUNEL assay was proceeded as described [23], the aortic arch was first detected by use of the DeadEnd Fluorometric TUNEL System (TB235, Promega, Fitchburg, WI, USA), then the aortic arch was stained with CD31 and DAPI. Fluorescence images were obtained using the Zeiss LSM700 (Carl Zeiss, Jena, Germany). Carl Zeiss ZEN 2010 program was used to measure the fluorescence intensity, which was measured in at least ten regions for each labeling condition, and representative results were shown.

Enzyme-linked immunosorbent assay (ELISA)

HMBOX1 WT and KO mouse were received an intraperitoneal injection of 20 mg/kg lipopolysaccharide (LPS) for 12 h, then the blood was harvested and centrifuged after euthanizing the mouse. TNF- α and IL-6 level in the mouse serum was measured using the TNF- α (BMS607-3, Invitrogen) and IL-6 (BMS603-2, Invitrogen) ELISA kits following the manufacturer's instructions.

Statistical analyses

All experiments were repeated at least 6 times independently. The data were expressed as the means \pm SEM and were analyzed by one-way ANOVA using SPSS v17.0 (SPSS Inc., Chicago, IL, USA). Images were processed using GraphPad Prism 7.00 (GraphPad Software, La Jolla, CA, USA) and Adobe Photoshop CC 14.0 (Adobe, San Jose, CA, USA). P-values less than 0.05 were regarded as statistically significant.

Results

The protein level of HMBOX1 is increased during mouse development

We first examined HMBOX1 protein levels in several major tissues of FVB/N mouse at day 1, 3, 7, 14, 21, 28 and 56,

respectively. The results from western blot showed that the expression of HMBOX1 was very low at day 1, but then gradually increased from day 3 to day 56 in the heart, liver, spleen, kidney and brain (Fig. 1). These results indicated that HMBOX1 might play a key function in mouse development.

Generation of TALEN-mediated HMBOX1 knockout mice

In order to illustrate the influence of HMBOX1 on mouse development and the maintenance of EC functions. The HMBOX1 knockout (KO) mouse was generated using

TALENs-mediated gene inactivation. A pair of TALEN constructs was created that specifically targeted HMBOX1 exon 3, immediately downstream of the start of translation (Supplementary Fig. S1A). The DNA sequencing results from tail DNA revealed that there was 10-bp (5'-ACCATGTCCTC-3') deletion in HMBOX1 knockout mouse, we confirmed the mutation from the sequencing of knockout mouse liver mRNA (Fig. 2a, b, Supplementary Fig. S1B). The mutated mouse was predicted to create a frameshift mutation after translating 11 amino acids.

We next investigated whether functional HMBOX1 protein production was truly disrupted in the KO mouse. As

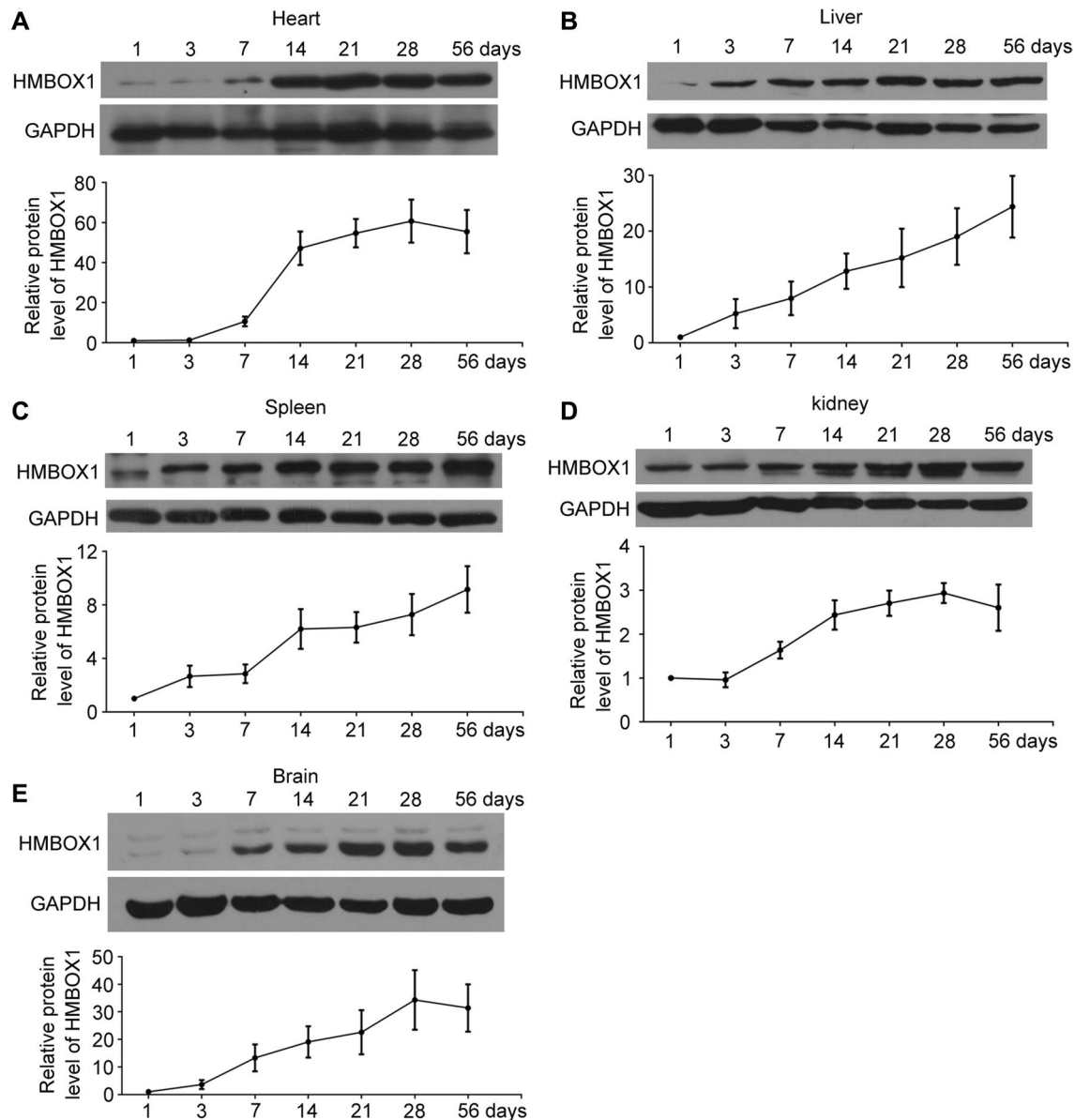
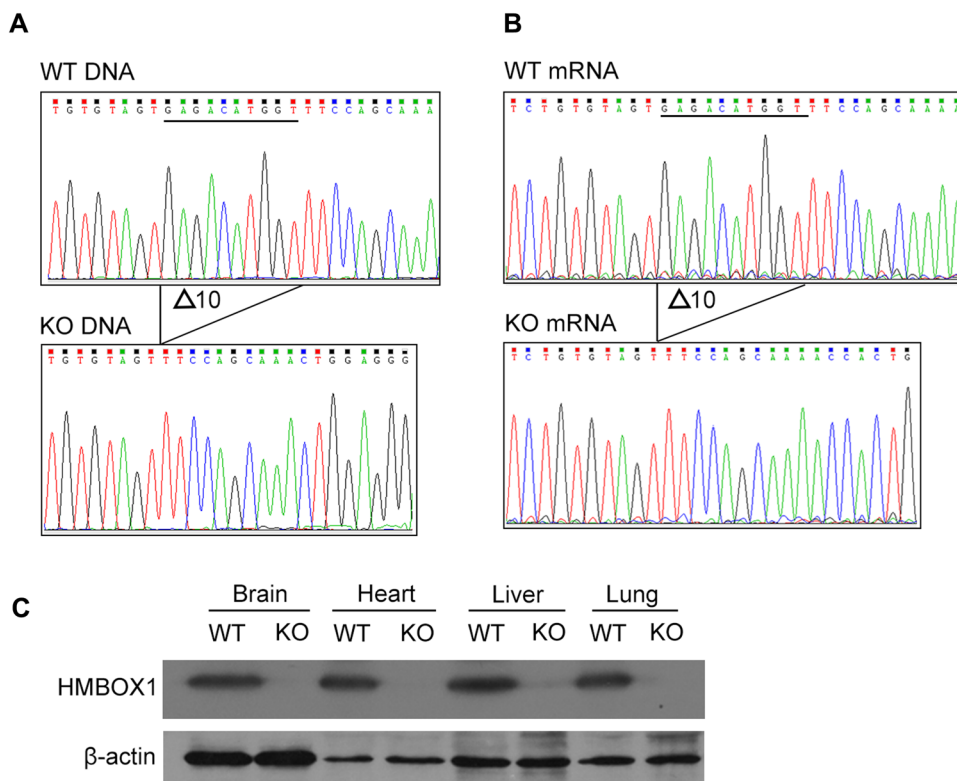


Fig. 1 The expression of HMBOX1 during mouse development. The heart, liver, spleen, kidney and brain tissues were taken from FVB/N mouse at day 1, 3, 7, 14, 21, 28 and 56, respectively. The protein levels of HMBOX1 and GAPDH were detected by western blot. $n=6$

Fig. 2 Validation of the deletion of HMBOX1 in knockout mouse. **a** DNA sequencing chromatograms of WT and KO mouse tails from genomic DNA PCR products, demonstrating the 10-bp deletion in the KO sample. **b** DNA sequencing chromatograms of WT and KO mouse from liver mRNA RT-PCR products. **c** Western blot analysis of protein levels of HMBOX1 and β -actin in brain, heart, liver, lung tissues of WT and KO mouse



shown in Fig. 2c, HMBOX1 protein was undetectable in the brain, heart, liver and lung tissues of HMBOX1 KO mouse. To further confirm that 10 nucleotide deletions in HMBOX1 KO mouse could break the expression of HMBOX1, we cloned the wild type (WT) and mutant coding sequences of HMBOX1 into the pEGFP-C2 expression vector to construct pEGFP-C2-WT and pEGFP-C2-KO plasmids. The protein of HMBOX1 was normally expressed in HEK293T cells transfected with pEGFP-C2-WT, while cells transfected with pEGFP-C2-KO failed to translate normal HMBOX1 protein (Supplementary Fig. S2).

The HMBOX1 KO mouse was fertile and could breed normally, with no obvious abnormalities. Although studies emphasized the essential role of HMBOX1 in supporting telomere maintenance *in vitro*, the loss of HMBOX1 did not affect the lifespan of the mouse within the time frame we observed (2 years). Collectively, these results indicated that loss of HMBOX1 did not arrest mouse development.

Loss of HMBOX1 increases apoptosis of aortic endothelial cells under LPS treatment

Our previous studies showed that knockdown of HMBOX1 promoted apoptosis of HUVECs [19], so we next investigate whether HMBOX1 deletion influence EC survival in mouse. However, we failed to detect an increased number of apoptotic endothelial cell in normal-fed HMBOX1 KO mice (Figs. 3a, 4a). Besides, in mouse brain tissue sections, we

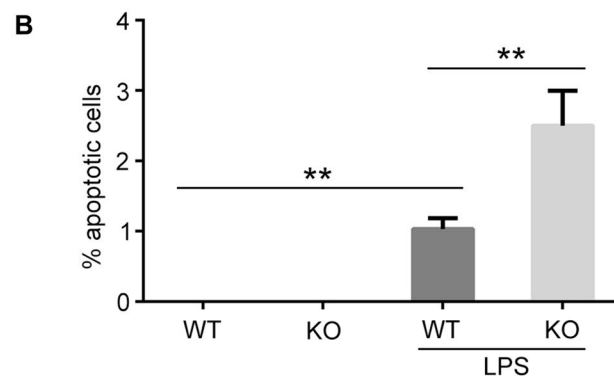
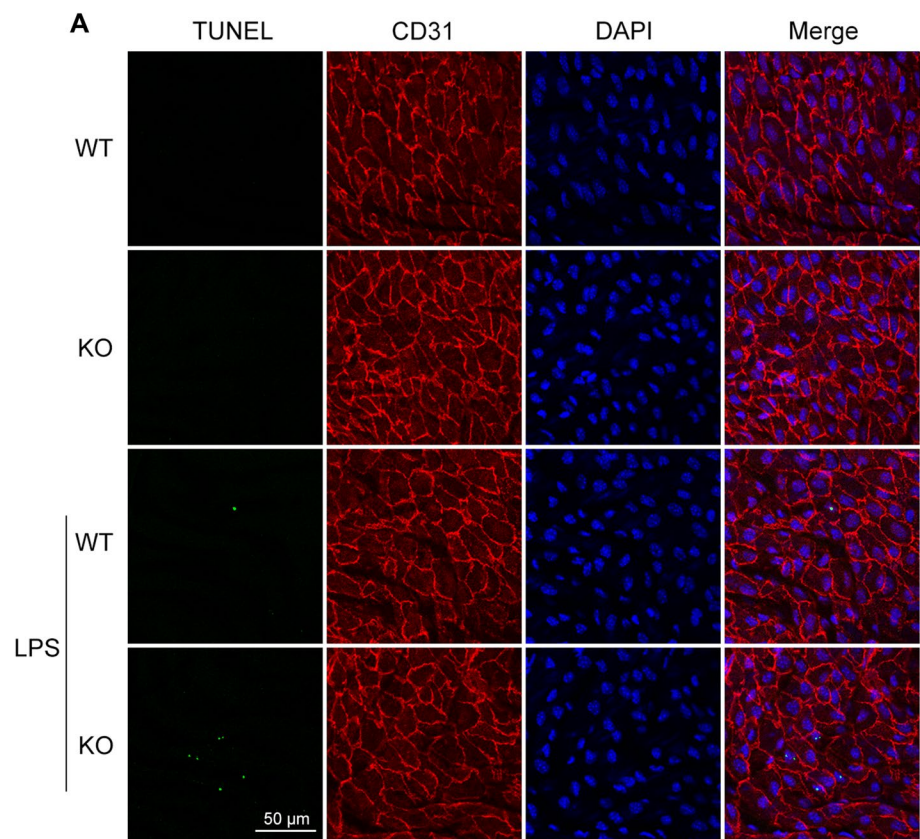
also did not observe significant differences in vessel density and length between WT and KO mouse (Supplementary Fig. S3).

Subsequently, we examined the apoptosis of aortic endothelial cells in WT and KO mice under the stimulation of lipopolysaccharide (LPS), a well-known apoptosis-inducing agent. TUNEL staining showed that no apoptosis was detected in aortic endothelial cells of WT and KO mouse without LPS treatment. However, the apoptosis rate of aortic endothelial cells in KO mice was significantly higher than that in WT mice after receiving an intraperitoneal injection of LPS (20 mg/kg) for 12 h (Fig. 3). Enface staining detection of cleaved caspase-3 suggested that the activation of caspase-3 in aortic endothelial cells of KO mice was significantly higher than that of WT mice under LPS stimulation, with no differences in control groups (Fig. 4). These results indicated that deletion of HMBOX1 reduced the ability of mouse aortic endothelial cells to resist external stimuli. Apoptosis was more likely to occur under LPS stimulation without HMBOX1 in mouse.

Loss of HMBOX1 inhibits autophagy of aortic endothelial cells under LPS treatment

Our previous studies have shown that knockdown of HMBOX1 could inhibit vascular endothelial cell autophagy [19]. Next, we examined the autophagy of aortic endothelial cells in HMBOX1 WT and KO mice under

Fig. 3 HMBOX1 deletion enhances the apoptosis of endothelium under LPS treatment. HMBOX1 WT and KO mouse were received an intraperitoneal injection of 20 mg/kg LPS for 12 h, then the aortic arch was dissected. **a** TUNEL assay was conducted to detect the apoptosis of aortic arch. CD31 and DAPI represented endothelium and nuclei, respectively. **b** The proportion of apoptosis in (a) was quantified. Scale bars: 50 μ m. $**p < 0.01$, $n = 6$

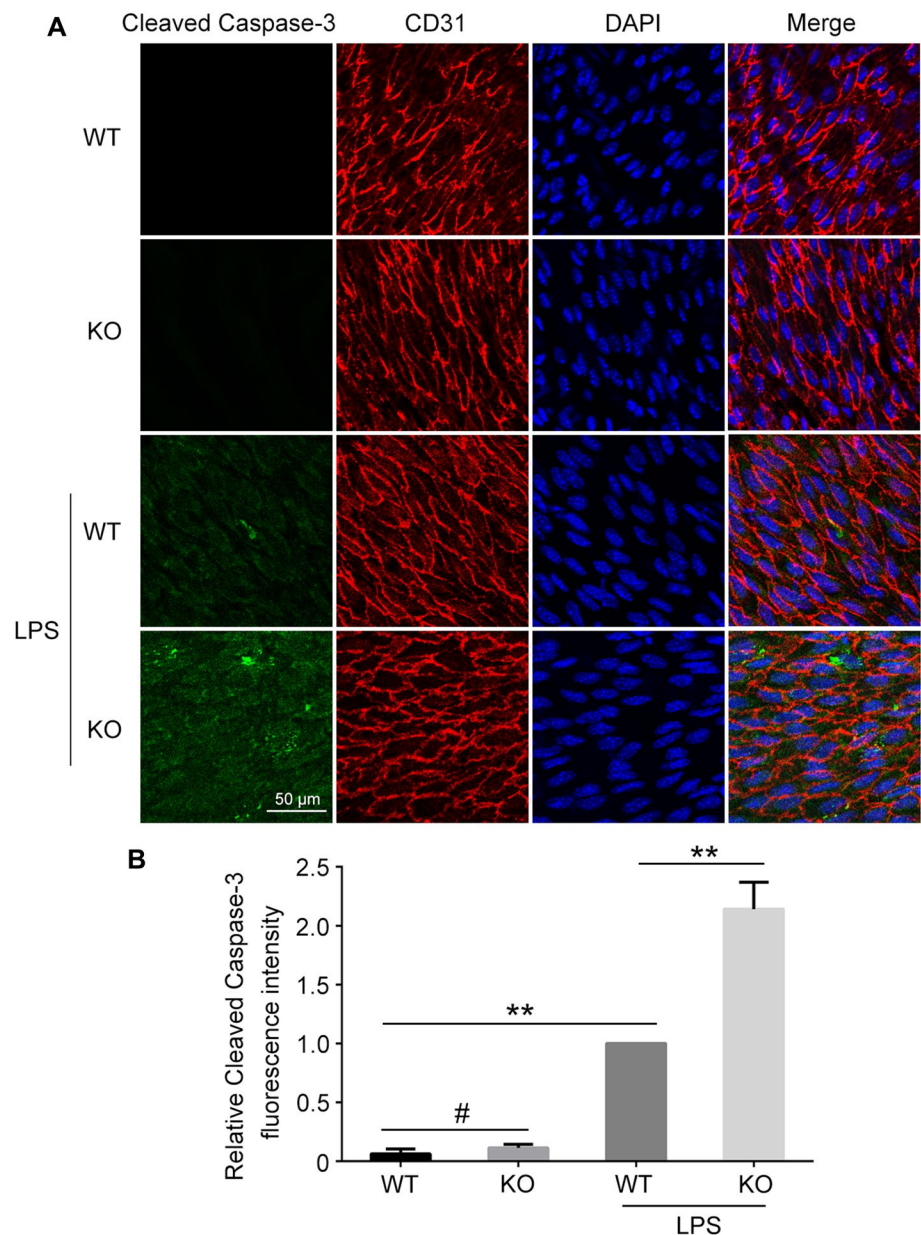


LPS stimulation. Enface staining showed that there was no significant difference in LC3B punctate aggregation of aortic endothelial cells between WT and KO mice in normal conditions. The punctate aggregation of LC3B in WT and KO mice was significantly increased after intraperitoneal injection of LPS (20 mg/kg) for 12 h, but the dot-like aggregation of LC3B in KO mice was apparently lower than that in WT mice (Fig. 5). These data indicated that HMBOX1 deletion impaired autophagic mobilization ability of aortic endothelial cells under LPS stimulation.

HMBOX1 deletion does not affect the expression of inflammatory factors under LPS stimulation

A recent study in hepatocyte-specific HMBOX1 knockout mice revealed that the decrease of HMBOX1 in hepatocytes enhanced the expression of inflammatory factors TNF- α and IL-6 [6]. We next investigated whether HMBOX1 whole-body knockout affected inflammatory factor expression. ELISA assay showed that HMBOX1 whole-body knockout did not affect the expression of inflammatory factors

Fig. 4 The level of cleaved caspase-3 was increased in HMBOX1 KO mouse under LPS treatment. HMBOX1 WT and KO mouse were received an intraperitoneal injection of 20 mg/kg LPS for 12 h, then the aortic arch was dissected. **a** En face staining was performed to detect the cleaved caspase-3 level in the aortic arch. CD31 and DAPI represented endothelium and nuclei, respectively. **b** The relative fluorescence intensity of cleaved caspase-3 in **(a)**. Scale bars: 50 μ m. # $p > 0.05$, ** $p < 0.01$, $n = 6$



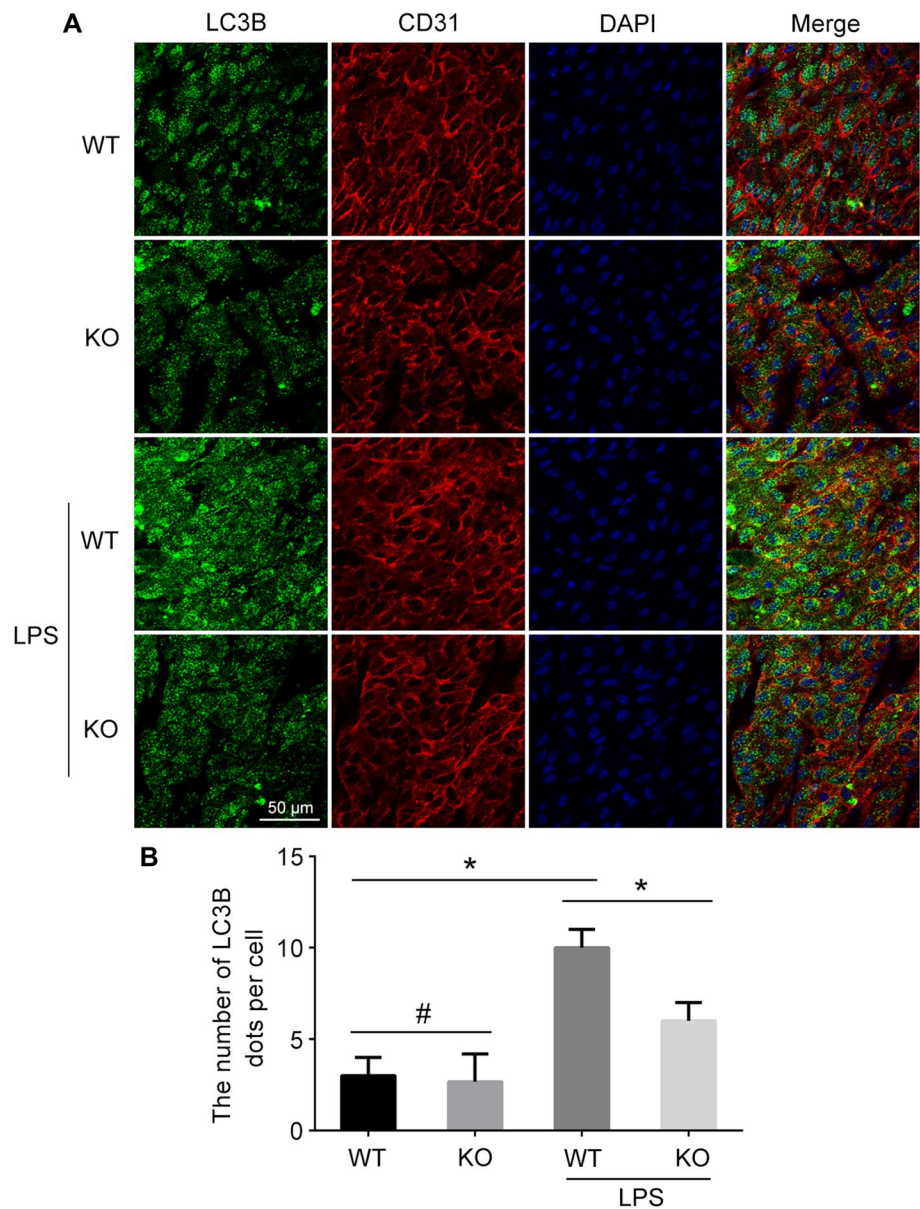
TNF- α and IL-6, whether under LPS stimulation or in the control groups (Fig. 6a). Furthermore, our results from cultured HAECs also suggested that LPS treatment significantly increased the levels of TNF- α and IL-6, but remained unchanged with HMBOX1 knockdown (Fig. 6b).

Effect of HMBOX1 on the expression of major pro-apoptotic genes

At the beginning of its discovery, HMBOX1 was proved to be a transcriptional repressor [1], so far, no target genes of

HMBOX1 had been reported. In view of the important role of HMBOX1 in regulating endothelial cell apoptosis in vitro and in vivo, we next turned to explore whether HMBOX1 directly regulated the expression of several major pro-apoptotic genes. We overexpressed or disrupted HMBOX1 in HEK293T cells by transfecting the plasmid pCMV6-HMBOX1 containing the full-length HMBOX1 cDNA or HMBOX1 siRNA (80 nm), and detected the mRNA level of HMBOX1, BCL-2, BAX, BAD, BID, caspase-3, caspase-8, caspase-9, PARP1. The results indicated that HMBOX1 had no significant effect on the expression of these genes (Fig. 6c).

Fig. 5 HMBOX1 deletion attenuates the autophagy of endothelium under LPS treatment. HMBOX1 WT and KO mouse were received an intraperitoneal injection of 20 mg/kg LPS for 12 h, then the aortic arch was dissected. **a** En face staining was performed to detect the LC3B dots in the aortic arch. CD31 and DAPI represented endothelium and nuclei, respectively. **b** The number of LC3B dots per cell in (a) was quantified. Scale bars: 50 μ m. # $p > 0.05$, * $p < 0.05$, $n = 6$



Discussion

The homeodomain-containing proteins, encoded by homeobox genes, are a superfamily of transcription factors that play important roles in genetic control of development and angiogenesis [21, 24–26]. The phylogenetic comparison reveals that HMBOX1 belongs to the hepatocyte nuclear factors (HNF) subclass, but shares only 28% and 27% sequence similarity to HNF1 α and HNF1 β , indicating that HMBOX1 may represent a distinct group of HNF [1]. Many homeobox genes-null models have been constructed to illustrate the function of these genes in mouse. In current study, in order to investigate the roles of HMBOX1 in mouse development and endothelium in vivo, we generated HMBOX1 whole-body knockout mouse by using TALENs technology for the first

time. Although the protein level of HMBOX1 was gradually increased during mouse development, HMBOX1 KO mouse was viable and fertile, and the loss of HMBOX1 did not affect the lifespan of mouse in the time frame we observed (2 years). This might be due to the fact that HMBOX1 is not a gene essential for mouse survival and reproduction. In addition, we observed no differences in the apoptosis and autophagy of aortic endothelial cells between WT and KO mouse under normal feeding conditions.

LPS is a component of the outer wall of gram-negative bacteria, and is the major reason accounting for sepsis [27]. In endothelial cells, exposure to LPS leads to endothelial activation through a receptor complex consisting of TLR4, CD14 and MD2, accompanied by recruitment of the adaptor protein MyD88 and activation of NF- κ B and MAPK signal

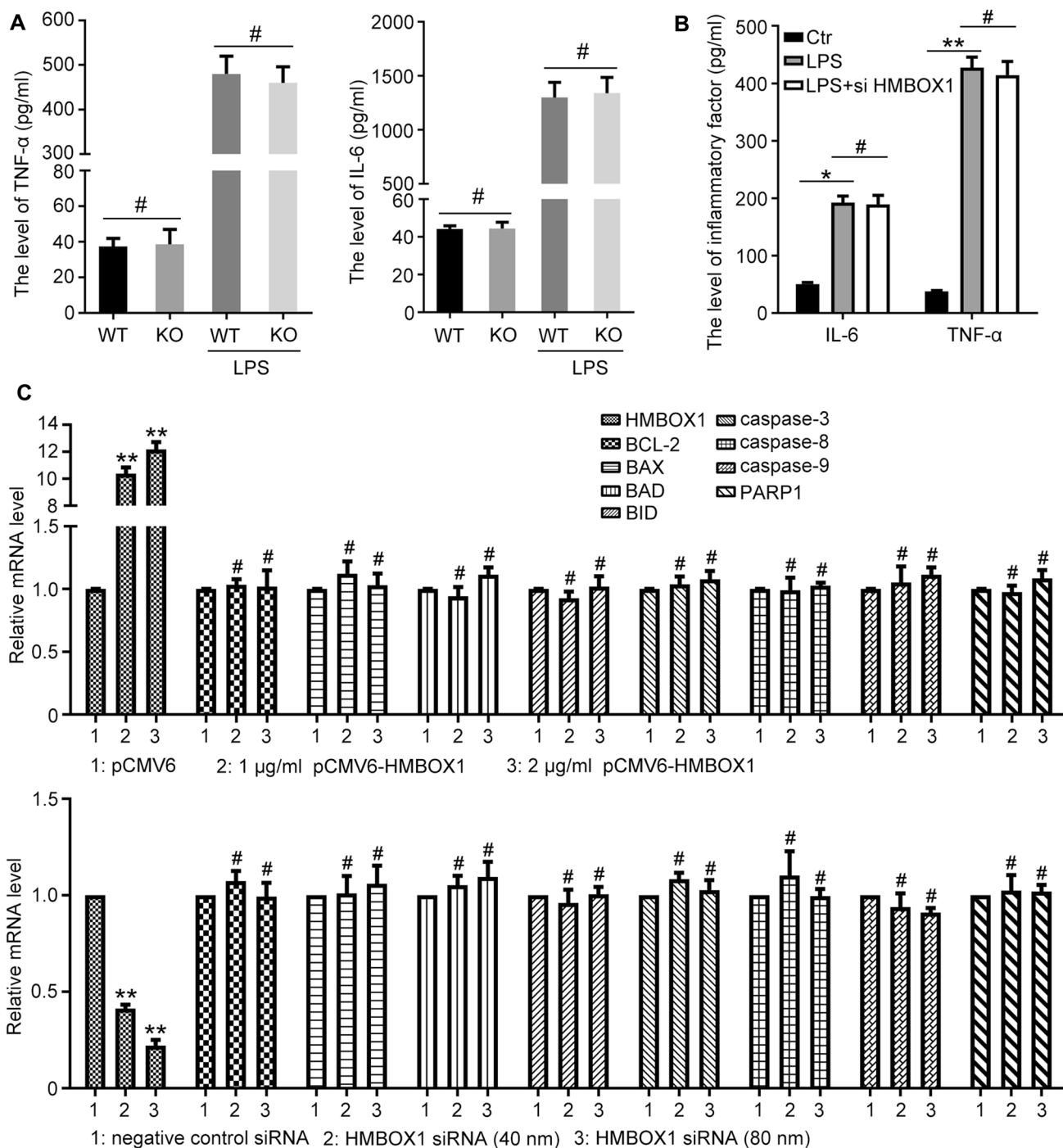


Fig. 6 Effect of HMBOX1 on the secretion of inflammatory cytokine and the expression of apoptosis-related genes. **a** HMBOX1 WT and KO mouse were received an intraperitoneal injection of 20 mg/kg LPS for 12 h. The level of TNF-α and IL-6 in mouse serum was measured by ELISA assay. #*p*>0.05, n=6. **b** HAECs were transfected with negative control siRNA or HMBOX1 siRNA (80 nm) for 24 h, followed by treatment with LPS (2 μg/ml) for 24 h, the level of

TNF-α and IL-6 in the supernatant was measured by ELISA assay. **c** qPCR analysis of the mRNA level of HMBOX1, BCL-2, BAX, BAD, BID, caspase-3, caspase-8, caspase-9 and PARP1 in HAECs cells transfected with empty vector pCMV6, pCMV6-HMBOX1 or negative control siRNA, HMBOX1 siRNA for 48 h. #*p*>0.05, **p*<0.05, ***p*<0.01, n=3

pathway, which ultimately promotes the production of various pro-inflammatory mediators and cellular injury [28–30]. Studies based on experiments in mice have shown that intraperitoneal injection of LPS could cause acute lung injury and endothelial cell apoptosis [31]. Our previous study found that LPS can induce autophagy in HUVECs through BIRC2 [32]. Besides, administration of LPS for 4 h could induce LC3 punctate aggregation in venular ECs in vivo [33, 34]. Thus, in this study, LPS was used to investigate the function of endothelial cells in HMBOX1 KO mouse.

LPS causes a decrease in intracellular free zinc level, thereby inducing apoptosis in cultured sheep pulmonary artery endothelial cells (SPAECs). In the meantime, elevation of exogenous zinc could counteract LPS induced apoptosis by promoting Zrt/Irt-like protein 14 (ZIP14) expression, which could be blocked by knockdown of metallothionein (MT), a zinc-binding protein [35–37]. Our previous study revealed that HMBOX1 regulated intracellular free zinc level by interacting with metallothionein 2A (MT2A) to inhibit apoptosis and promote autophagy in HUVECs [19]. In current study, we demonstrated that loss of HMBOX1 caused increased apoptosis and decreased autophagy of aortic endothelial cells with LPS treatment. These results indicated that, although HMBOX1 deletion failed to result in the death of mouse, as well as the abnormal of aortic endothelial cell differentiation and development, loss of HMBOX1 may destroy the intracellular zinc ion homeostasis of endothelial cells, thereby promoting apoptosis and inhibiting autophagy when stimulated by LPS. As our results obtained from HUVECs [19], the increased autophagy may mediate resistance to apoptosis induced by LPS in mouse.

Yuan et al. reported that HMBOX1, activated by 5,2'-dibromo-2,4',5'- trihydroxydiphenylmethanone (TDD), inhibited LPS-induced inflammation and ROS production in EA.hy926 cells by the subsequent inhibition of redox-sensitive NF- κ B and MAPK activation [5]. A study from hepatocyte-specific HMBOX1 KO mice suggested that the decrease of HMBOX1 promoted the activation of macrophages and upregulated the secretion of inflammatory factors (TNF- α and IL-6) under LPS/D-GalN stimulation [6]. However, in this research, we found that loss of HMBOX1 had no effect on the level of TNF- α and IL-6 in the serum of HMBOX1 whole-body knockout mouse and HAECs. We speculated that this may be due to other members of the homeobox family compensated for the role of HMBOX1, and this required further investigation. This result also indicated that the difference in apoptosis and autophagy occurring in WT and KO mice is not due to the stimulation by different levels of inflammatory factors.

Although years of research have shown that HMBOX1, a proven transcriptional repressor, plays key roles in tumorigenesis, telomere length maintenance, VEC differentiation and inflammatory response, no target genes of HMBOX1

have been reported until now. Herein, we tried to explore whether HMBOX1 regulated the expression of several key genes involved in apoptosis. Unfortunately, the results indicated that HMBOX1 had no significant effect on the expression of these genes. Thus, the increased apoptosis of endothelial cells could not be attributed to upregulated pro-apoptosis genes induced by HMBOX1 deletion.

Collectively, in this study, we constructed an HMBOX1 KO mouse using TALENs technology, and this model was used to investigate the role of HMBOX1 in the maintenance of mouse aortic endothelial cell function. Our results indicated that HMBOX1 deletion affected the anti-stress ability of mouse aortic endothelial cells. Apoptosis was more likely to occur when stimulated by LPS in KO mouse, and the level of autophagy was lower than that of WT mouse. HMBOX1 might be an important factor in regulating the function of endothelial cells in vivo.

Acknowledgements This work was financially supported by National Natural Science Foundation of China (Grant Nos. 31870831, 91539105, 81321061, 81902656), and the Shandong Provincial Natural Science Foundation (Grant No. ZR2019BH059).

Author contributions MH conceived of the presented idea, designed and performed the experiments, analyzed the data, carried out data interpretation, designed the figures, wrote the paper. SL performed the experiments, analyzed the data, carried out data interpretation. HX performed the experiments. MJ conceived and designed the experiments, supervised the work. All authors read and approved the final version of this manuscript.

Compliance with ethical standards

Conflicts of interest The authors declare no conflicts of interest.

Ethical approval All experimental procedures and animal care were performed in accordance with the ARRIVE guidelines [38] and approved by the ethics committee of Shandong University.

References

1. Chen S, Saiyin H, Zeng X, Xi J, Liu X, Li X, Yu L (2006) Isolation and functional analysis of human HMBOX1, a homeobox containing protein with transcriptional repressor activity. *Cytogenet Genome Res* 114(2):131–136. <https://doi.org/10.1159/000093328>
2. Wu L, Zhang C, Zhang J (2011) HMBOX1 negatively regulates NK cell functions by suppressing the NKG2D/DAP10 signaling pathway. *Cell Mol Immunol* 8(5):433–440. <https://doi.org/10.1038/cmi.2011.20>
3. Wu L, Zhang C, Zheng X, Tian Z, Zhang J (2011) HMBOX1, homeobox transcription factor, negatively regulates interferon-gamma production in natural killer cells. *Int Immunopharmacol* 11(11):1895–1900. <https://doi.org/10.1016/j.intimp.2011.07.021>
4. Gong J, Liu R, Zhuang R, Zhang Y, Fang L, Xu Z, Jin L, Wang T, Song C, Yang K, Wei Y, Yang A, Jin B, Chen L (2012) miR-30c-1* promotes natural killer cell cytotoxicity against human hepatoma cells by targeting the transcription factor

- HMBOX1. *Cancer Sci* 103(4):645–652. <https://doi.org/10.1111/j.1349-7006.2012.02207.x>
5. Yuan HX, Feng XE, Liu EL, Ge R, Zhang YL, Xiao BG, Li QS (2019) 5,2'-dibromo-2,4',5'-trihydroxydiphenylmethanone attenuates LPS-induced inflammation and ROS production in EA.hy926 cells via HMBOX1 induction. *J Cell Mol Med* 23(1):453–463. <https://doi.org/10.1111/jcmm.13948>
 6. Zhao H, Han Q, Lu N, Xu D, Tian Z, Zhang J (2018) HMBOX1 in hepatocytes attenuates LPS/D-GalN-induced liver injury by inhibiting macrophage infiltration and activation. *Mol Immunol* 101:303–311. <https://doi.org/10.1016/j.molimm.2018.07.021>
 7. Feng X, Luo Z, Jiang S, Li F, Han X, Hu Y, Wang D, Zhao Y, Ma W, Liu D, Huang J, Songyang Z (2013) The telomere-associated homeobox-containing protein TAH1/HMBOX1 participates in telomere maintenance in ALT cells. *J Cell Sci* 126(Pt 17):3982–3989. <https://doi.org/10.1242/jcs.128512>
 8. Kappei D, Butter F, Benda C, Scheibe M, Draskovic I, Stevense M, Novo CL, Basquin C, Araki M, Araki K, Krastev DB, Kitzler R, Jessberger R, Londono-Vallejo JA, Mann M, Buchholz F (2013) HOT1 is a mammalian direct telomere repeat-binding protein contributing to telomerase recruitment. *EMBO J* 32(12):1681–1701. <https://doi.org/10.1038/emboj.2013.105>
 9. Tarsounas M (2013) It's getting HOT at telomeres. *EMBO J* 32(12):1655–1657. <https://doi.org/10.1038/emboj.2013.119>
 10. Zhang P, Liu Q, Yan S, Yuan G, Shen J, Li G (2017) Homeobox-containing protein 1 loss is associated with clinicopathological performance in glioma. *Mol Med Rep* 16(4):4101–4106. <https://doi.org/10.3892/mmr.2017.7050>
 11. Zhou J, Wang M, Deng D (2018) c-Fos/microRNA-18a feedback loop modulates the tumor growth via HMBOX1 in human gliomas. *Biomed Pharm* 107:1705–1711. <https://doi.org/10.1016/j.biopha.2018.08.157>
 12. Yu YL, Diao NN, Li YZ, Meng XH, Jiao WL, Feng JB, Liu ZP, Lu N (2018) Low expression level of HMBOX1 in high-grade serous ovarian cancer accelerates cell proliferation by inhibiting cell apoptosis. *Biochem Biophys Res Commun* 501(2):380–386. <https://doi.org/10.1016/j.bbrc.2018.04.203>
 13. Zhao H, Jia H, Han Q, Zhang J (2018) Homeobox containing 1 inhibits liver cancer progression by promoting autophagy as well as inhibiting stemness and immune escape. *Oncol Rep* 40(3):1657–1665. <https://doi.org/10.3892/or.2018.6551>
 14. Diao N, Li Y, Yang J, Jin C, Meng X, Jiao W, Feng J, Liu Z, Lu N (2019) High expression of HMBOX1 contributes to poor prognosis of gastric cancer by promoting cell proliferation and migration. *Biomed Pharm* 115:108867. <https://doi.org/10.1016/j.biopha.2019.108867>
 15. Zhou S, Xiao Y, Zhuang Y, Liu Y, Zhao H, Yang H, Xie C, Zhou F, Zhou Y (2017) Knockdown of homeobox containing 1 increases the radiosensitivity of cervical cancer cells through telomere shortening. *Oncol Rep* 38(1):515–521. <https://doi.org/10.3892/or.2017.5707>
 16. Su L, Zhao H, Sun C, Zhao B, Zhao J, Zhang S, Su H, Miao J (2010) Role of Hmbox1 in endothelial differentiation of bone-marrow stromal cells by a small molecule. *ACS Chem Biol* 5(11):1035–1043. <https://doi.org/10.1021/cb100153r>
 17. Han L, Shao J, Su L, Gao J, Wang S, Zhang Y, Zhang S, Zhao B, Miao J (2012) A chemical small molecule induces mouse embryonic stem cell differentiation into functional vascular endothelial cells via Hmbox1. *Stem Cells Dev* 21(15):2762–2769. <https://doi.org/10.1089/scd.2012.0055>
 18. Ma H, Su L, Zhang S, Kung H, Miao J (2016) Inhibition of ANXA7 GTPase activity by a small molecule promotes HMBOX1 translation of vascular endothelial cells in vitro and in vivo. *Int J Biochem Cell Biol* 79:33–40. <https://doi.org/10.1016/j.biocel.2016.08.010>
 19. Ma H, Su L, Yue H, Yin X, Zhao J, Zhang S, Kung H, Xu Z, Miao J (2015) HMBOX1 interacts with MT2A to regulate autophagy and apoptosis in vascular endothelial cells. *Scientific reports* 5:15121. <https://doi.org/10.1038/srep15121>
 20. Burglin TR, Affolter M (2016) Homeodomain proteins: an update. *Chromosoma* 125(3):497–521. <https://doi.org/10.1007/s00412-015-0543-8>
 21. Holland PW (2013) Evolution of homeobox genes. *Wiley Interdiscip Rev* 2(1):31–45. <https://doi.org/10.1002/wdev.78>
 22. Ma H, Li Y, Wang X, Wu H, Qi G, Li R, Yang N, Gao M, Yan S, Yuan C, Kong B (2019) PBK, targeted by EVI1, promotes metastasis and confers cisplatin resistance through inducing autophagy in high-grade serous ovarian carcinoma. *Cell Death Dis* 10(3):166. <https://doi.org/10.1038/s41419-019-1415-6>
 23. Nowak-Sliwinska P, Alitalo K, Allen E, Anisimov A, Aplin AC, Auerbach R, Augustin HG, Bates DO, van Beijnum JR, Bender RHF, Bergers G, Bikfalvi A, Bischoff J, Bock BC, Brooks PC, Bussolino F, Cakir B, Carmeliet P, Castranova D, Cimpean AM, Cleaver O, Coukos G, Davis GE, De Palma M, Dimberg A, Dings RPM, Djonov V, Dudley AC, Dufton NP, Fendt SM, Ferrara N, Fruttiger M, Fukumura D, Ghesquiere B, Gong Y, Griffin RJ, Harris AL, Hughes CCW, Hultgren NW, Iruela-Arispe ML, Irving M, Jain RK, Kalluri R, Kalucka J, Kerbel RS, Kitajewski J, Klaassen I, Kleinmann HK, Koolwijk P, Kuczyński E, Kwak BR, Marien K, Melero-Martin JM, Munn LL, Nicosia RF, Noel A, Nurro J, Olsson AK, Petrova TV, Pietras K, Pili R, Pollard JW, Post MJ, Quax PHA, Rabinovich GA, Raica M, Randi AM, Ribatti D, Ruegg C, Schlingemann RO, Schulte-Merker S, Smith LEH, Song JW, Stacker SA, Stalin J, Stratman AN, Van de VM, van Hinsbergh, Vermeulen VWM, Waltenberger PB, Weinstein J, Xin BM, Yetkin-Arik H, Yla-Herttuala B, Yoder S, Griffioen MC AW (2018) Consensus guidelines for the use and interpretation of angiogenesis assays. *Angiogenesis* 21(3):425–532. <https://doi.org/10.1007/s10456-018-9613-x>
 24. Kachgal S, Mace KA, Boudreau NJ (2012) The dual roles of homeobox genes in vascularization and wound healing. *Cell Adhes Migr* 6(6):457–470. <https://doi.org/10.4161/cam.22164>
 25. He B, Ni ZL, Kong SB, Lu JH, Wang HB (2018) Homeobox genes for embryo implantation: from mouse to human. *Anim Models Exp Med* 1(1):14–22. <https://doi.org/10.1002/ame2.12002>
 26. Procino A (2016) Class I homeobox genes, "The Rosetta Stone of the Cell Biology", in the regulation of cardiovascular development. *Curr Med Chem* 23(3):265–275
 27. Pfalzgraff A, Weindl G (2019) Intracellular lipopolysaccharide sensing as a potential therapeutic target for sepsis. *Trends Pharmacol Sci* 40(3):187–197. <https://doi.org/10.1016/j.tips.2019.01.001>
 28. Yang WS, Kim JJ, Lee MJ, Lee EK, Park SK (2018) ADAM17-mediated ectodomain shedding of toll-like receptor 4 as a negative feedback regulation in lipopolysaccharide-activated aortic endothelial cells. *Cell Physiol Biochem* 45 (5):1851–1862. <https://doi.org/10.1159/000487876>
 29. Yao Y, Jia H, Wang G, Ma Y, Sun W, Li P (2019) miR-297 Protects human umbilical vein endothelial cells against LPS-induced inflammatory response and apoptosis. *Cell Physiol Biochem* 52 (4):696–707. <https://doi.org/10.33594/000000049>
 30. Dayang EZ, Plantinga J, Ter Ellen B, van Meurs M, Molema G, Moser J (2019) Identification of LPS-activated endothelial subpopulations with distinct inflammatory phenotypes and regulatory signaling mechanisms. *Front Immunol* 10:1169. doi:<https://doi.org/10.3389/fimmu.2019.01169>
 31. Ogata-Suetsugu S, Yanagihara T, Hamada N, Ikeda-Harada C, Yokoyama T, Suzuki K, Kawaguchi T, Maeyama T, Kuwano K, Nakanishi Y (2017) Amphiregulin suppresses epithelial cell apoptosis in lipopolysaccharide-induced lung injury in mice. *Biochem Biophys Res Commun* 484(2):422–428. <https://doi.org/10.1016/j.bbrc.2017.01.142>

32. Meng N, Wu L, Gao J, Zhao J, Su L, Su H, Zhang S, Miao J (2010) Lipopolysaccharide induces autophagy through BIRC2 in human umbilical vein endothelial cells. *J Cell Physiol* 225(1):174–179. <https://doi.org/10.1002/jcp.22210>
33. Pickworth CM, Beal R, Reglero N, Lintermans L, Colom B, Voisin M-B, Golding M, Nourshargh S (2016) Microvascular endothelial cells can exhibit autophagy in vivo: role in neutrophil transendothelial cell migration? *FASEB J* 30(1 Supplement):165-8
34. Zhang D, Zhou J, Ye LC, Li J, Wu Z, Li Y, Li C (2018) Autophagy maintains the integrity of endothelial barrier in LPS-induced lung injury. *J Cell Physiol* 233(1):688–698. <https://doi.org/10.1002/jcp.25928>
35. Thambiayya K, Wasserloos K, Kagan VE, Stoyanovsky D, Pitt BR (2012) A critical role for increased labile zinc in reducing sensitivity of cultured sheep pulmonary artery endothelial cells to LPS-induced apoptosis. *Am J Physiol Lung Cell Mol Physiol* 302(12):L1287–L1295. doi:<https://doi.org/10.1152/ajplung.00385.2011>
36. Thambiayya K, Kaynar AM, St Croix CM, Pitt BR (2012) Functional role of intracellular labile zinc in pulmonary endothelium. *Pulm Circ* 2(4):443–451. <https://doi.org/10.4103/2045-8932.105032>
37. Thambiayya K, Wasserloos KJ, Huang Z, Kagan VE, St Croix CM, Pitt BR (2011) LPS-induced decrease in intracellular labile zinc, [Zn]_i, contributes to apoptosis in cultured sheep pulmonary artery endothelial cells. *Am J Physiol Lung Cell Mol Physiol* 300(4):L624–L632. doi:<https://doi.org/10.1152/ajplung.00376.2010>
38. Kilkenny C, Browne WJ, Cuthill IC, Emerson M, Altman DG (2010) Improving bioscience research reporting: the ARRIVE guidelines for reporting animal research. *PLoS Biol* 8(6):e1000412. <https://doi.org/10.1371/journal.pbio.1000412>

Publisher's Note Springer Nature remains neutral with regard to jurisdictional claims in published maps and institutional affiliations.